

Directed Assembly of DNA-Functionalized Gold Nanoparticles Using Pyrrole–Imidazole Polyamides

Željka Krpetić,^{†,||} Ishwar Singh,[‡] Wu Su,[§] Luca Guerrini,[†] Karen Faulds,[†] Glenn A. Burley,^{*,‡} and Duncan Graham^{*,†}

[†]Centre for Molecular Nanometrology, WestCHEM, Department of Pure and Applied Chemistry, The University of Strathclyde, 295 Cathedral Street, Glasgow G1 1XL, United Kingdom

[‡]Department of Pure and Applied Chemistry, WestCHEM, The University of Strathclyde, 295 Cathedral Street, Glasgow G1 1XL, United Kingdom

[§]Department of Chemistry, The University of Leicester, University Road, Leicester LE1 7RH, United Kingdom

S Supporting Information

ABSTRACT: Traditional methods for the construction of nanoparticle arrays and lattices exploit Watson–Crick base pairing of single-stranded DNA sequences as a proxy for self-assembly. Although this approach has been utilized in a variety of applications in nanoassembly, diagnostics, and biomedicine, the diversity of this recognition lexicon could be considerably increased by developing strategies that recognize the base-pairing landscape of double-stranded DNA (dsDNA) sequences. Herein we describe the first report of programmed gold nanoparticle (GNP) aggregation directed by the recognition of dsDNA sequences using pyrrole–imidazole polyamide–GNP (PA–GNP) conjugates. We demonstrate the reversibility and selectivity of this strategy for forming GNP aggregates in the presence of fully matched dsDNA sequences relative to dsDNA sequences containing one- and two-base-pair mismatches.

Nucleic acids are a powerful tool for the programmable bottom-up construction of nanoscale arrays.^{1–5} By virtue of their predictable self-assembling properties,⁶ the recognition of single-stranded DNA (ssDNA) sequences by their molecular complements is an established modality for the directed assembly of nanoscale materials such as metal nanoparticles (NPs),¹ semiconducting quantum dots,^{2,7} and biocompatible NPs.⁸ In this respect, programmable self-assembly is achieved by the recognition of the primary sequences of ssDNA via the direct readout of Watson–Crick base-pairing regimes. The predictable and reproducible recognition properties of ssDNA sequences for their molecular complements have found utility as a fundamental tool in nanoassembly,^{3,9} as a platform for applications in diagnostics^{1,10–13} and imaging,^{14,15} and in the development of biomedical materials manipulation of biological processes¹⁶ such as gene expression.^{17–22} An underexploited modality for the directed assembly of nanomaterials is the exploitation of alternative structural features such as B-type DNA duplexes.²³ The structure of B-DNA consists of a periodic array of major and minor grooves where the edges of the hydrogen-bond donor and acceptor groups of each Watson–Crick base pair provide a readout mechanism equivalent to that

of direct hybridization.²⁴ An exemplary small-molecule exponent of this type of recognition is the family of molecules known as pyrrole–imidazole polyamides (PAs).²⁵ PAs are synthetic oligomers that bind within the minor groove of DNA to target sequences up to 12 base pairs in length. Their mode of DNA binding is specific for dsDNA and has recently been exploited in the construction of nanoscale assemblies along DNA architectures such as proteins,^{26,27} DNA nanorings,^{28–31} and small-molecule fluorophores.³² To date, however, there have been no investigations of their potential to direct the assembly of metal NPs. Here we present the directed assembly/disassembly of gold NPs (GNPs) using PA–GNP conjugates. We demonstrate the programmability and thermodynamics of PA–GNP conjugates to induce an aggregation process that is both reversible and sequence-dependent.

The principal aims of this study were twofold: first, to develop a synthetic protocol for the preparation of PA-functionalized GNPs (PA–GNP1), and second, to determine whether PA–GNP1 would direct an aggregation process in the presence of a target dsDNA sequence. In our design, the 5'-end of a DNA strand is attached to a different GNP (GNP2, Figure 1) via thiol–gold linkages. The addition of its molecular complement forms a dsDNA duplex on the GNP surface (i.e., GNP2 or GNP4), and this enables one to screen the recognition landscape of PA–GNP1 expediently by the simple addition of a series of single-stranded oligo-(deoxyribonucleotide) (ODN) sequences. PA 1 (Figure 1) was chosen as an exemplar sequence to test this hypothesis, as its core is known to bind to the seven-base-pair DNA sequence 5'WWGWWCW (W = A/T) with a binding constant in the nanomolar regime (Figure 1a).³³ The synthesis of 1 [section S1 in the Supporting Information (SI)] was achieved by using Boc-based solid-phase synthetic methodology^{34,35} followed by resin cleavage with *N*1-3-aminopropyl-*N*1-methylpropane-1,3-diamine to give PA 2, on which the dithiol–triethylene glycol acid was then installed via amide coupling to afford 1 in 76% yield. The triethylene glycol bridge³⁶ between the lipoic acid moiety and the PA core imparts sufficient water solubility to the system and maintains an appropriate distance and flexibility

Received: February 24, 2012

Published: May 7, 2012

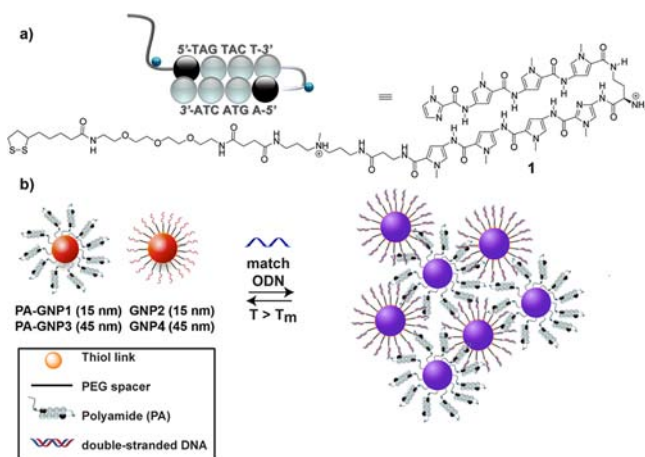


Figure 1. (a) Sequence of PA 1. (b) Scheme of 1- and ssDNA-functionalized GNPs and their subsequent aggregation upon addition of DNA matching sequences (ODNs).

between the surface of GNP1 and the core recognition sequence of PA 1.

The preparation of PA-GNPs with different core sizes was carried out to investigate the influence of NP size on the colorimetric and spectroscopic response of dsDNA recognition.³⁷ An optimized synthetic protocol was developed for the preparation of PA-GNPs that avoids particle aggregation due to the high affinity of the lone pairs of the imidazole units toward the GNP surface (section S2).³⁸ A two-step ligand exchange preparation method involving initial passivation of the GNP surface by physisorption of a nonionic surfactant (Tween 20) followed by the addition of 1 was devised.³⁹ Tween 20 mediates the exchange of citrate anions on the GNP surface and 1 by sterically shielding the GNP surface prior to the addition of 1.⁴⁰ Using this approach, we prepared stable PA-GNP1 conjugates with a 100% loading of 1. Confirmation of the attachment of 1 to the GNP surface was verified using differential centrifugal sedimentation (CPS), which confirmed a shift in the mean diameter of PA-GNPs relative to unfunctionalized GNP versions as a consequence of the changes in both the hydrodynamic drag of the ligand monolayer and the overall nanoparticle density (section S3).⁴¹ The estimated numbers of ligands per particle were 4000 and 35600 for 15 and 45 nm GNPs, respectively, as determined using ICP-AES (section S3).

The capacity of free PA 1 to bind to its target sequence 5'-WWGWWCW was then investigated using isothermal binding measurements.⁴² The 13-mer ODN duplex ODN1 comprising a single 1 target sequence 5'-TAG TAC T-3' exhibited a 9.7 °C stabilization of the duplex melting temperature (ΔT_m ; Table S2 in the SI). The sequence selectivity of 1 for this binding site relative to the duplex ODN2 containing a one-base-pair mismatch (5'-AGT AGT AAG CAG C-3') resulted in a significant decrease in the stabilization of the duplex melting temperature ($\Delta T_m = 4$ °C). The introduction of an additional mismatch destabilized T_m even further, but the magnitude of this destabilization was highly dependent on the location of these two mismatches within the context of the target sequence (ODN3–5; Table S2). These results confirm that 1 binds to its target sequence with both high affinity and selectivity. To assess the capacity of PA-GNP1 to direct the assembly of 15 nm GNPs, an ssDNA-stabilized GNP (GNP2) was prepared via thiolation of the surface of citrate-coated GNPs with a thiol-

modified ODN (5'-SS-ODN) using a variation of an established salt-aging method⁴³ and then characterized using Centrifugal Particle Sizing (CPS) (section S3). We hypothesized that the PA component of PA-GNP1 would direct the aggregation of GNP2 only in the presence of the complementary ODN probe strand ODN1. To investigate this assumption, we performed a series of melting point experiments utilizing the characteristic surface plasmon resonance (SPR) peak of GNPs at 520 nm as a diagnostic marker of aggregation. As a result of reversible aggregation of the particles, a sharp decrease in the extinction at 520 nm along with a red shift in the SPR was evidenced only in the presence of all three components, namely, PA-GNP1, GNP2, and ODN1 (Figure 2). Much akin to conventional

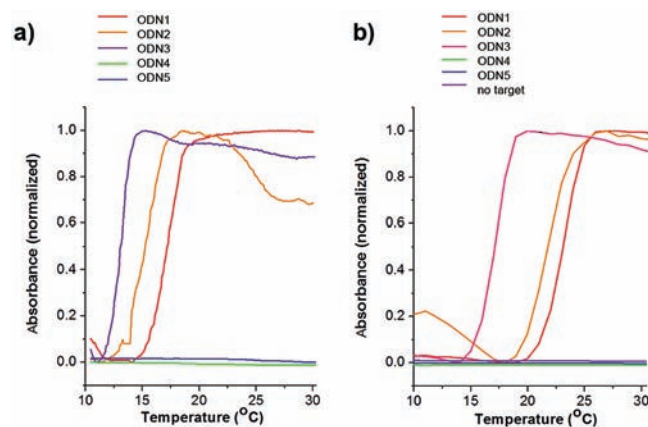


Figure 2. Melting curves in the presence of ODN1–5 on (a) 15 and (b) 45 nm diameter PA-GNPs and Au-ODN NPs.

particle aggregation mediated by the hybridization of complementary ssODN sequences,¹ a sharp T_m was also observed at 17 °C for the fully matching DNA sequence ODN1 over a 60 °C temperature range (Figure 2). No T_m was observed in the absence of ODN1 (section S5) or in the presence of a “nonsense” DNA target sequence, thus confirming the selectivity of PA-GNP1 binding only to dsDNA.²⁵ Transmission electron microscopy (TEM) images of the fully matched PA-GNP1 system in the presence of GNP2 and ODN1 confirmed the nature of the interaction as an aggregation process (Figure 3).

The T_m profiles in the presence of one-base-pair (ODN2) and two-base-pair (ODN3 and ODN4) mismatched probes were depressed by 2–4 °C relative to the fully matched ODN1 system (Figure 2). Because of the sharpness of the melting curves, the matched versions were easily differentiated from one- and two-base-pair mismatches. In this respect, for

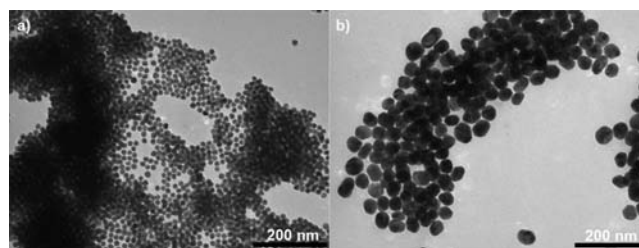


Figure 3. TEM micrographs of aggregation events occurring between PA-GNPs and Au-ODN NPs in the presence of target DNA sequence ODN1: (a) 15 and (b) 45 nm diameter.

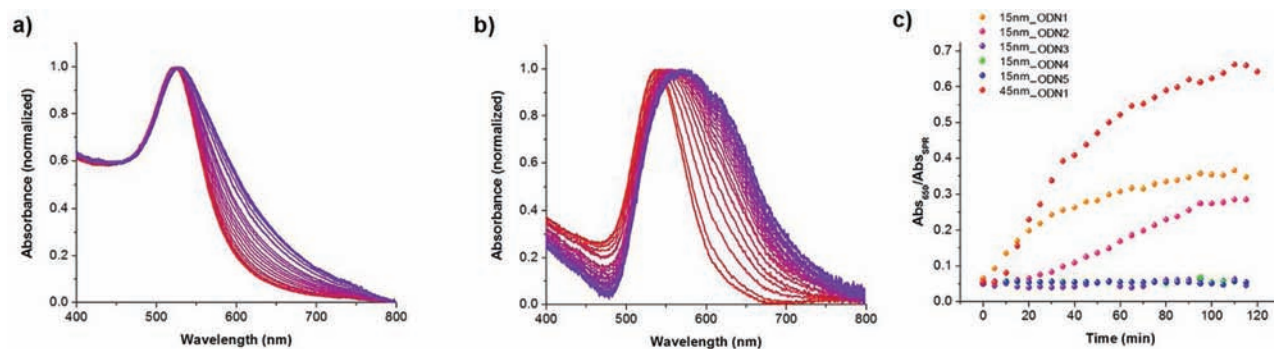


Figure 4. Aggregation of the PA–GNPs in the presence of DNA-functionalized GNPs followed by UV–vis spectroscopy (scanning kinetics at 10 °C) upon addition of the fully matched target DNA sequence ODN1 over 120 min. A colorimetric response was observed for (a) 15 and (b) 45 nm GNPs. (c) Aggregation chart for comparison of the size- and DNA-sequence-dependent colorimetric responses, reported as Abs_{650}/Abs_{SPR} ratios.

example, a 2 °C decrease in T_m was observed for ODN2 relative to the matched version. Much akin to the melting studies conducted using unmodified DNA duplexes (Figure S18 in the SI), T_m was highly sensitive to the location of the two base-pair mismatches within the duplex. An exemplar of this is the observation of a complete loss of a T_m when the two-base-pair mismatch resided toward the 5/3' end of the PA binding sequence (Figure 2a). A similar trend in T_m was also observed for the aggregation profiles of 45 nm PA–GNP3 and GNP4 with the matched and one- and two-base-pair-mismatched probe strands. A key difference in this system was a 5–7 °C increase in T_m values relative to the 15 nm PA–GNP1 versions. This increase in T_m is commensurate with previous observations on a purely DNA-based GNP system⁴⁴ and is assumed to be a consequence of more extensive contact surface area available in larger GNPs. The rate of GNP aggregation was assessed by a 7 nm red shift of the SPR peak over 40 min for the 15 nm PA–GNP series (Figure 4a). The one-base-pair-mismatched PA–GNP1 system resulted in a significantly lower rate of aggregation relative to the matched system, according to a plot of the Abs_{650}/Abs_{SPR} ratio as a function of time (Figure 4c). This trend of increased rate of aggregation (38 nm red shift) in the presence of matched dsDNA was also reflected in the 45 nm GNP series (Figure 4b), although the onset of the aggregation process was slower for the matched 45 nm PA–GNP3 version than for the 15 nm PA–GNP1.

Plasmonic coupling of GNPs that are in close proximity generates intense electromagnetic fields at the interparticle junctions, providing a strong enhancement of the Raman scattering from molecules located at or near the interparticle gap.⁴⁵ To assess the PA-driven aggregation via surface-enhanced Raman spectroscopy (SERS), DNA-functionalized GNPs (GNP2) were covalently labeled with a near-IR dye (NIR-797, $\lambda_{ex} = 795$ nm). Laser excitation at 785 nm was selected for the SERS experiments to maximize the scattering efficiency of the resonant Raman reporter NIR-797 [surface-enhanced resonant Raman scattering (SERRS) was observed under our experimental conditions].⁴⁶ Dye-labeled Au–ODN NPs showed an appreciable Raman signal with an extremely low surface coverage of the reporter molecule, thus avoiding perturbation of the DNA ligand monolayer.³⁷ The intensity of the SERRS signal was highly dependent on the aggregation state (Figure 5a). As a consequence of the duplex formation and further linkage with PA–GNPs at low temperatures (Figure 5b, 10 °C), the SERRS intensity underwent a marked

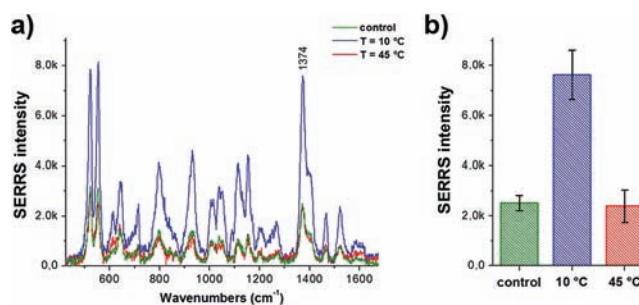


Figure 5. (a) Baseline-corrected SERRS spectra of NIR-797 and (b) corresponding SERRS intensities of the 1374 cm^{-1} band in the absence (green) and in the presence of the ODN1 target sequence at 10 °C (blue) and 45 °C (red). Error bars represent standard deviations from three repetitions.

increase relative to the monodispersed particle system (Figure 5b, control). Conversely, when the temperature was raised above T_m (Figure 5b, 45 °C), the SERRS signal dropped to its original value corresponding to the nonaggregated system. As foreseen, in the case of smaller core size GNPs, no significant changes in the SERRS intensity were observed upon particle aggregation because of the much poorer enhancing abilities of 15 nm diameter GNP clusters in comparison with the larger ones.³⁷ Colorimetric detection of ODN1 offered higher sensitivity with 45 nm core size GNPs than with 15 nm diameter GNPs [limit of detection (LOD) = 10^{-9} and 10^{-8} M, respectively; section S11].³⁷ This is the first example of temperature-dependent selective “on/off” switching of a SERRS response involving dye-labeled DNA-functionalized GNPs directed by reversible particle assembly in the presence of PA–GNPs and the matching target DNA sequence. Our SERS data fully support the colorimetric and T_m results.

In conclusion, we have described a new concept for the directed assembly of GNPs controlled by the recognition capabilities of PAs to bind to dsDNA sequences selectively. This is the first example of such a process programmed by the recognition of dsDNA using GNPs tethered with minor-groove-binding PA ligands. As the vast majority of DNA in biological systems is present in double-stranded form, our study provides a proof of concept that PA–GNP conjugates can read out dsDNA sequences directly, thereby dispelling the need for time-consuming denaturation steps required in conventional DNA detection assays. In our proof-of-concept study, we used an eight-ring PA exemplar and demonstrated its capacity to recognize a seven-base-pair dsDNA recognition sequence

immobilized on a GNP surface. It is known that the length of target dsDNA sequences of PAs can be tuned according to the number of pyrrole and imidazole units. It is therefore feasible that sequences much longer than the seven-base-pair ones highlighted in this study could be recognized, as reported previously with free polyamides.^{47,48} We therefore envision new applications in a number of areas, such as the selective recognition of unique and biologically relevant dsDNA sequences and single-nucleotide polymorphisms in biodiagnostics as well as in structural DNA nanotechnology.

■ ASSOCIATED CONTENT

● Supporting Information

PA synthesis, purification, and characterization; preparation and surface modification of GNPs; characterization of GNPs by TEM, CPS, and ICP-AES; dependence of PA-GNP-mediated aggregation on the complementarity of the DNA probe strand; control experiments; SERRS experiments; ¹H and ¹³C NMR spectra; ESI-MS and HPLC data; MALDI-MS analysis; melting experiments; and LOD measurements. This material is available free of charge via the Internet at <http://pubs.acs.org>.

■ AUTHOR INFORMATION

Corresponding Author

glenn.burley@strath.ac.uk; duncan.graham@strath.ac.uk

Present Address

^{||}Department of Chemistry, The University of Liverpool, Liverpool L69 7ZD, United Kingdom (Z.K.).

Notes

The authors declare no competing financial interest.

■ ACKNOWLEDGMENTS

The authors greatly acknowledge Prof. Mathias Brust and Dr. Ian A. Prior (The University of Liverpool) for access to the EM Unit Facility and the use of the CPS centrifuge, the EPSRC for an Advanced Research Fellowship to G.A.B. (EP/E055095/1) and a postdoctoral fellowship to W.S. (EP/G048878/1), and the Royal Society for a Wolfson Research Merit Award to D.G.

■ REFERENCES

- (1) Rosi, N. L.; Mirkin, C. A. *Chem. Rev.* **2005**, *105*, 1547.
- (2) Choi, C. L.; Alivisatos, A. P. *Annu. Rev. Phys. Chem.* **2010**, *61*, 369.
- (3) Park, S. Y.; Lytton-Jean, A. K. R.; Lee, B.; Weigand, S.; Schatz, G. C.; Mirkin, C. A. *Nature* **2008**, *451*, 553.
- (4) Travesset, A. *Science* **2011**, *334*, 183.
- (5) Tan, S. J.; Campolongo, M. J.; Luo, D.; Cheng, W. *Nat. Nanotechnol.* **2011**, *6*, 268.
- (6) Auyeung, E.; Cutler, J. I.; Macfarlane, R. J.; Jones, M. R.; Wu, J.; Liu, G.; Zhang, K.; Osberg, K. D.; Mirkin, C. A. *Nat. Nanotechnol.* **2012**, *7*, 24.
- (7) Tikhomirov, G.; Hooglang, S.; Lee, P. E.; Fischer, A.; Sargent, E. H.; Kelley, S. O. *Nat. Nanotechnol.* **2011**, *6*, 485.
- (8) Dave, N.; Liu, J. *ACS Nano* **2011**, *5*, 1304.
- (9) Nykypanchuk, D.; Maye, M. M.; van der Lelie, D.; Gang, O. *Nature* **2008**, *451*, 549.
- (10) Tan, Y. N.; Lee, K. H.; Su, X. *Anal. Chem.* **2011**, *83*, 4251.
- (11) Garcia, T.; Casero, E.; Revenga-Parra, M.; Pariente, F.; Lorenzo, E. *Anal. Chem.* **2008**, *80*, 9443.
- (12) Zanchet, D.; Micheel, C. M.; Parak, W. J.; Gerion, D.; Alivisatos, A. P. *Nano Lett.* **2000**, *1*, 32.
- (13) Lee, K.; Drachev, V. P.; Irudayaraj, J. *ACS Nano* **2011**, *5*, 2109.
- (14) Song, Y.; Xu, X.; MacRenaris, K. W.; Zhang, X. Q.; Mirkin, C. A.; Meade, T. J. *Angew. Chem., Int. Ed.* **2009**, *48*, 9143.
- (15) Jayagopal, A.; Halfpenny, K. C.; Perez, J. W.; Wright, D. W. *J. Am. Chem. Soc.* **2010**, *132*, 9789.
- (16) Coomber, D.; Bartczak, D.; Gerrard, S. R.; Tyas, S.; Kanaras, A. G.; Stulz, E. *Langmuir* **2010**, *26*, 13760.
- (17) Dhar, S.; Daniel, W. L.; Giljohann, D. A.; Mirkin, C. A.; Lippard, S. J. *J. Am. Chem. Soc.* **2009**, *131*, 14652.
- (18) Rosi, N. L.; Giljohann, D. A.; Thaxton, C. S.; Lytton-Jean, A. K. R.; Mirkin, C. A. *Science* **2006**, *312*, 1027.
- (19) Prigodich, A. E.; Alhasan, A. H.; Mirkin, C. A. *J. Am. Chem. Soc.* **2011**, *133*, 2120.
- (20) Lee, S. E.; Lee, L. P. *Curr. Opin. Chem. Biol.* **2010**, *14*, 623.
- (21) Giljohann, D. A.; Seferos, D. S.; Prigodich, A. E.; Patel, P. C.; Mirkin, C. A. *J. Am. Chem. Soc.* **2009**, *131*, 2072.
- (22) Seferos, D. S.; Giljohann, D. A.; Hill, H. D.; Prigodich, A. E.; Mirkin, C. A. *J. Am. Chem. Soc.* **2007**, *129*, 15477.
- (23) Su, W.; Bonnard, V.; Burley, G. A. *Chem.—Eur. J.* **2011**, *17*, 7982.
- (24) Endo, M.; Sugiyama, H. *ChemBioChem* **2009**, *10*, 2420.
- (25) Dervan, P. B.; Edelson, B. S. *Curr. Opin. Struct. Biol.* **2003**, *13*, 284.
- (26) Cohen, J. D.; Sadowski, J. P.; Dervan, P. B. *J. Am. Chem. Soc.* **2008**, *130*, 402.
- (27) Cohen, J. D.; Sadowski, J. P.; Dervan, P. B. *Angew. Chem., Int. Ed.* **2007**, *46*, 7956.
- (28) Schmidt, T. L.; Heckel, A. *Nano Lett.* **2011**, *11*, 1739.
- (29) Ackermann, D.; Rasched, G.; Verma, S.; Schmidt, T. L.; Heckel, A.; Famulok, M. *Chem. Commun.* **2010**, *46*, 4154.
- (30) Schmidt, T. L.; Heckel, A. *Small* **2009**, *5*, 1517.
- (31) Schmidt, T. L.; Nandi, C. K.; Rasched, G.; Parui, P. P.; Brutschy, B.; Famulok, M.; Heckel, A. *Angew. Chem., Int. Ed.* **2007**, *46*, 4382.
- (32) Su, W.; Schuster, M.; Bagshaw, C. R.; Rant, U.; Burley, G. A. *Angew. Chem., Int. Ed.* **2011**, *50*, 2712.
- (33) Trauger, J. W.; Baird, E. E.; Dervan, P. B. *Nature* **1996**, *382*, 559.
- (34) Su, W.; Gray, S. J.; Dondi, R.; Burley, G. A. *Org. Lett.* **2009**, *11*, 3910.
- (35) Baird, E. E.; Dervan, P. B. *J. Am. Chem. Soc.* **1996**, *118*, 6141.
- (36) Kanaras, A. G.; Kamounah, F. S.; Schaumburg, K.; Kiely, C. J.; Brust, M. *Chem. Commun.* **2002**, 2294.
- (37) Krpetić, Ž.; Guerrini, L.; Larmour, I. A.; Reglinski, J.; Faulds, K.; Graham, D. *Small* **2012**, *8*, 707.
- (38) Souza, G. R.; Levin, C. S.; Hajitou, A.; Pasqualini, R.; Arap, W.; Miller, J. H. *Anal. Chem.* **2006**, *78*, 6232.
- (39) Aslan, K.; Pérez-Luna, V. H. *Langmuir* **2002**, *18*, 6059.
- (40) Duy, J.; Connell, L. B.; Eck, W.; Collins, S. D.; Smith, R. L. *J. Nanopart. Res.* **2010**, *12*, 2363.
- (41) Krpetić, Ž.; Nativo, P.; Prior, I. A.; Brust, M. *Small* **2011**, *7*, 1982.
- (42) Dose, C.; Farkas, M. E.; Chenoweth, D. M.; Dervan, P. B. *J. Am. Chem. Soc.* **2008**, *130*, 6859.
- (43) McKenzie, F.; Faulds, K.; Graham, D. *Chem. Commun.* **2008**, 2367.
- (44) Hurst, S. J.; Hill, H. D.; Mirkin, C. A. *J. Am. Chem. Soc.* **2008**, *130*, 12192.
- (45) Halas, N. J.; Lal, S.; Chang, W.-S.; Link, S.; Nordlander, P. *Chem. Rev.* **2011**, *111*, 3913.
- (46) Smith, W. E. *Chem. Soc. Rev.* **2008**, *37*, 955.
- (47) Brunett, R.; Melander, C.; Puckett, J. W.; Son, L. S.; Wells, R. D.; Dervan, P. B.; Gottesfeld, J. M. *Proc. Natl. Acad. Sci. U.S.A.* **2006**, *103*, 11497.
- (48) (a) Turner, J. M.; Baird, E. E.; Dervan, P. B. *J. Am. Chem. Soc.* **1997**, *119*, 7636. (b) Swalley, S. E.; Baird, E. E.; Dervan, P. B. *Chem.—Eur. J.* **1997**, *3*, 1600. (c) Trauger, J. W.; Baird, E. E.; Dervan, P. B. *J. Am. Chem. Soc.* **1998**, *120*, 3534. (d) Herman, D. M.; Baird, E. E.; Dervan, P. B. *Chem.—Eur. J.* **1999**, *5*, 975.